Metal enhanced fluorescence on nanoporous gold leaf-based assay platform for virus detection

Syed Rahin Ahmed [a,b], Md. Ashraf Hossain [b], Jung Youn Park [c], Soo-Hyung Kim [b], Dongyun Lee [d], Tetsuro Suzuki [e], Jaebeom Lee [d,*], Enoch Y. Park [a,f,**]

[a] Graduate School of Science and Technology, Shizuoka University, 836 Ohya Suruga-ku, Shizuoka 422-8529, Japan
[b] Department of Nano Fusion Technology, Pusan National University, Miryang 627-706, Republic of Korea
[c] National Fisheries Research and Development Institute, Busan 619-705, Republic of Korea
[d] Department of Nano Fusion Engineering and Cogno-Mechatronics Engineering, Pusan National University, Busan 609-735, Republic of Korea
[e] Department of Infectious Diseases, Hamamatsu University School of Medicine, 1-20-1 Higashi-ku, Handa-yama, Hamamatsu 431-3192, Japan
[f] Research Institute of Green Science and Technology, Shizuoka University, 836 Ohya Suruga-ku, Shizuoka 422-8529, Japan

A R T I C L E I N F O

A B S T R A C T

In the present study, a rapid, sensitive and quantitative detection of influenza A virus targeting hemagglutinin (HA) was developed using hybrid structure of quantum dots (QDs) and nanoporous gold leaf (NPGL). NPGL film was prepared by dealloying bimetallic film where its surface morphology and roughness were fairly controlled. Anti-influenza A virus HA antibody (ab66189) was bound with NPGL and amine ($-NH_2$) terminated QDs. These biofunctionalized NPGL and QDs formed a complex with the influenza virus A/Beijing/262/95 (H1N1) and the photoluminescence (PL) intensities of QDs were linearly correlated with the concentrations of the virus up to 1 ng/mL while no PL was observed in the absence of the virus, or in bovine serum albumin (BSA, 1 μg/mL) alone. In addition, it was demonstrated that this assay detected successfully influenza virus A/Yokohama/110/2009 (H3N2) that is isolated from a clinical sample, at a concentration of ca. 50 plaque forming units (PFU)/mL. This detection limit is 2-order more sensitive than a commercially available rapid influenza diagnostic test. From these results, the proposed assay may offer a new strategy to monitor influenza virus for public health.

© 2014 Elsevier B.V. All rights reserved.

1. Introduction

Epidemic diseases via transmission of the virus are becoming a threatening fear for public health system; e.g., the pandemic influenza A (H1N1) 2009 virus was firstly identified in Mexico in 2009 and caused rapid outbreaks, resulting in ca. 18,000 casualties around the world (Kawai et al., 2012; Panning et al., 2009). It continues to expand globally and causes significant rates of morbidity and mortality, particularly in the elderly and children. A rapid diagnosis of influenza viruses is vital for prevention and timely control of influenza epidemics. Currently forefront tests, i.e.,

immunosensors and genosensors for monitoring influenza viruses at initial stage usually require professional skill, equipment, multiple processes, and low sensitivity, resulting in retardation to clinical decision (Bonanni et al., 2010; Choi et al., 2010; Deng et al., 2011; Drexler et al., 2009; Druce et al., 2005; Egashira et al., 2008; Kok et al., 2010; Kukol et al., 2008; Owen et al., 2007; Pavlovic et al., 2008; Rahman et al., 2008; van Elden et al., 2001). Numerous technologies for higher sensitivity are emerging for virus detection.

In particular, it has been attractive to utilize photoluminescence (PL) enhancement based on the near-field plasmonic effect at metallic nanostructures (Driskell et al., 2011; Gramotnev and Bozhevolnyi, 2010; Schuller et al., 2010). The interaction between metal and semiconductor nanostructure offers attractive opportunities for tuning the optical properties of such composites based on exciton–plasmon coupling. Such composite structures feature complementary optical properties; e.g., semiconductor nanostructures give rise to high emission yields and light-harvesting capabilities, whereas the metallic surface is particularly effective for local probing, confined excitation, non-linear optics and intense PL enhancement (Achermann, 2010; Lee et al., 2006, 2007). Surface roughness has long been considered as one of the

---

* Corresponding author. Tel.: +82 55 350 5298; fax: +82 55 350 5299.
** Corresponding author at: Research Institute of Green Science and Technology, Shizuoka University, 836 Ohya Suruga-ku, Shizuoka 422-8529, Japan.
Tel./fax: +81 54 238 4887.
E-mail addresses: rahin_sust@yahoo.com (S.R. Ahmed),
ashraf3521@gmail.com (Md.A. Hossain), jypark@nfrdi.go.kr (J.Y. Park),
sookim@pusan.ac.kr (S.-H. Kim), dlee@pusan.ac.kr (D. Lee),
tesuzuki@hama-med.ac.jp (T. Suzuki), jaebeom@pusan.ac.kr (J. Lee),
acypark@ipc.shizuoka.ac.jp, acypark@icloud.com (E.Y. Park).

critical parameters for optimizing metal enhanced fluorescence and has enabled precise control of localized surface plasmon resonance (LSPR) as well as surface plasmon polariton (SPP). In rough metallic surface, the scattering of SPP mode can produce photons that can decrease diffraction limit and resolve the sub-wavelength structure, thereby unlocking the prospect of utilizing metal–semiconductor nanocomposite films for enhancing PL emission (Ahmed et al., 2012; Leong et al., 2010; Okamoto et al., 2004).

Nanoporous gold film has unique physical properties such as excellent stability, biocompatibility, as well as high specific surface area to form self-assembled monolayers from thiols, sulfides and disulfides (Biener et al., 2008; Huang and Sun, 2005). Usually a dealloying technique is utilized to prepare nanoporous structures with controlled pore size and ligaments. By exploiting the dealloying method, PL enhancement in the vicinity of metal nanostructures can be achieved with delicate control of the morphology of the surface on the scale of a few hundreds nanometers in conjunction with interconnected-porous structures (Ciesielski et al., 2008; Detsi et al., 2011).

In the present study, the fabrication of metallic surfaces with tunable roughness and controlled structures is reported using the dealloying method. The procedure for fabrication of metal–semiconductor hybrid nanostructures was achieved by means of self-assembly techniques, and the importance of the metallic surface morphology for PL enhancement is illustrated. Furthermore, this physical study expanded to develop a highly sensitive metal–semiconductor hybrid nanostructure for the detection of influenza virus (Fig. 1).

2. Materials and methods

2.1. Materials

3-Mercaptopropionic acid (MPA; 99%), poly-diallyldimethylammonium chloride (PDDA; M.W. 400,000–500,000), polyacrylic acid (PAA; M.W.,∼450,000), cadmium perchlorate hydrate, thioglycolic acid (TGA), N-(3-dimethylaminopropyl)-N'-ethylcarbodiimide (EDC) and N-hydroxysuccinimide (NHS) were purchased from Sigma-Aldrich (Milwaukee, USA). Aluminum telluride (Al_2Te_3) was acquired from Cerac Company (Milwaukee, USA) at the highest purity available. The chromogenic substrate, 3,3′, 5,5′-tetramethylbenzidine (TMB) was obtained from Dojindo (Osaka, Japan). Gold leaf films were purchased from Giusto Manetti Inc. (Campi Bisenzio, Italy). Anti-Influenza A virus HA H1 antibody [B219M] (ab661189, Lot: GR40088-11), anti-Swine Influenza A (H1N1) HA antibody (ab91530, Lot: 942815), and anti-H3 (H3N2) antibody [InA227] (ab82454, Lot: GR84403-3) were purchased from Abcam Inc. (Cambridge, UK). Recombinant influenza A virus HA (H1N1) (New Caledonia/20/1999; Cat: 11683-V08H) and influenza virus A/Beijing/262/95 (H1N1) (Cat: 81N73-2) were purchased from Sino Biological Inc. (Beijing, China) and HyTest Lyd. (Turku, Finland), respectively. Influenza virus A/Yokohama/110/2009 (H3N2) that was isolated from a clinical sample was kindly provided by Dr. C. Kawakami of the Yokohama City Institute of Health, Japan, and was used for confirming the versatility of the assay system. ECL^{TM} anti-mouse IgG, horseradish peroxidase (HRP) linked whole antibody (from sheep) was purchased from GE Healthcare UK Ltd. (Buckinghamshire, UK). All other chemicals were obtained from Wako Pure Chem. Ind. Ltd. (Osaka, Japan). All experiments were carried out using high purity deionized (DI) water (> 18 MΩ).

2.2. Preparation of NPGL and semiconductor nanoparticles

The dealloying process of NPGL film has previously been described (Ciesielski et al., 2008). In this study, a gold/silver leaf was gently placed on a microscope slide. This slide was then slowly immersed into a beaker of concentrated nitric acid in order to float the leaf at the air–acid interface. The glass slide was removed when the leaf floated freely on the surface of the nitric acid solution. Subsequently, it was dealloyed for the desired time intervals of 5, 10, 30, and 60 min, and labeled as NPGL05, NPGL10, NPGL30 and NPGL60, respectively. The leaf was removed from the acid using a glass slide and transferred into a beaker containing deionized water, where the leaf was rinsed by floating for 30 min. The dealloyed leaf was withdrawn on a glass substrate that had
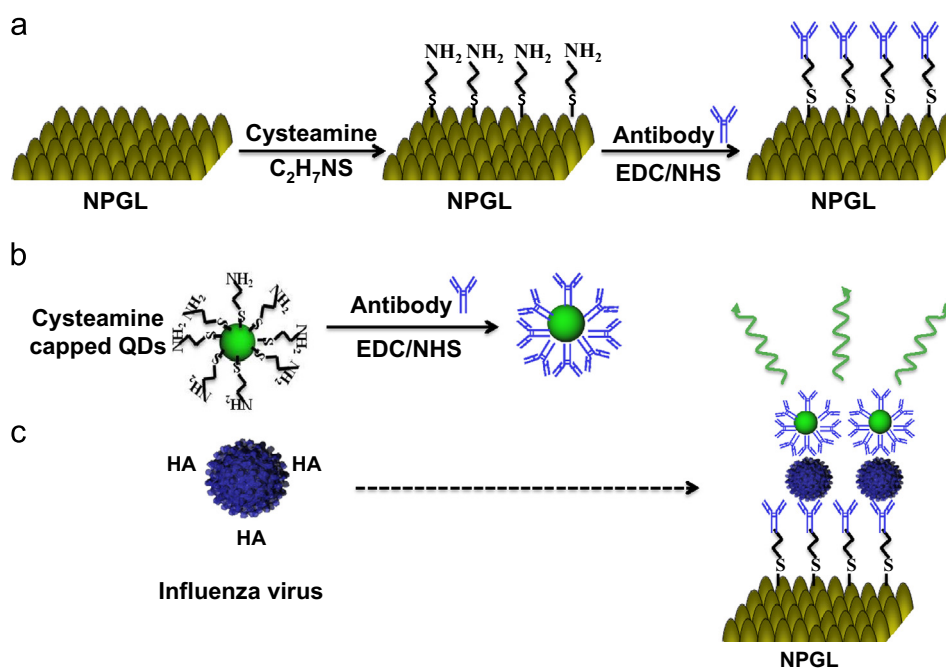
Fig. 1. Schematic of virus detection using nanoporous gold leaf (NPGL) film. The NPGL (a) and quantum dots (QDs) (b) were firstly conjugated with anti-hemagglutinin (HA) antibodies (anti-HA Ab, Y shape) by the reaction of ethylcarbodiimide (EDC)/N-hydroxysuccinimide (NHS). Then anti-HA Ab-conjugated with NPGL and QDs form complex (c) in presence of HA on the surface of influenza virus, finally enhancing PL intensity.

previously been modified with 3-mercaptopropyl trimethoxysilane in *n*-hexane. TGA-capped cadmium telluride (CdTe) QDs were also synthesized by a technique previously reported in detail (Gaponik et al., 2002) and stored at 4 °C prior to use.

2.3. Immobilization of CdTe QDs on the NPGL substrate

To evaluate optical properties of NPGL surface, the QDs were immobilized on the NPGL substrate by means of ultrasonic-assisted layer-by-layer (LbL) assembly (Ouyang et al., 2012; Perelshtein et al., 2008) (Supporting information S1). The polymer spacer layer of ca. 20 nm between nanocrystals and metal surface avoids unwanted quenching effects but assists PL enhancement.

2.4. Topographic observation and spectroscopic studies of NPGL films

Topographic images of the NPGL surfaces were obtained using atomic force microscopy (AFM, diInnova, Veeco, USA) and scanning electron microscopy (SEM, S4700, Hitachi High-Technol. Co., Minato-ku, Japan).

2.5. Detection platform of HA, Influenza viruses A/Beijing/262/95 (H1N1), and A/Yokohama/110/2009 (H3N2) on NPGL

Antibody specificity for HA (H1N1) was confirmed using an enzyme-linked immunosorbent assay (ELISA) (Supporting information S2) before conjugation to NPGL5 film. The anti-HA Ab (ab66189)-conjugated NPGL5 films (Supporting information S3) were rinsed 3 times with phosphate buffered saline (PBS). 100 μl anti-HA Ab-conjugated QDs (Ab-QDs) (Supporting information S1 and S4) containing different concentrations of recombinant influenza HA (H1N1) were added to the microplate wells. An Ab-QDs solution in BSA and without influenza virus HA (H1N1) was added to the same microplate as a negative control. To determine the PL enhancement effect of NPGL05 for HA detection, an identical amount of Ab-QDs solution containing 10 mg/mL HA protein was added to the wells of microplate. The microplate was

then incubated for 30 min at room temperature. An infinite® F500 microplate fluorescence reader (TECAN, Männedorf, Switzerland) was employed to measure the PL intensity of each well. The samples were excited at 380 nm, and the exciting and the emission slits were 5 and 10 nm, respectively. Based on the PL values at different concentrations of HA, a dose-dependent curve was constructed. This NPGL-based assay platform was applied on detection of two different types of influenza viruses using the same protocol as described above. Influenza virus A/Beijing/262/95 (H1N1) was detected using anti-HA (H1N1) Ab-bioconjugated NPGL and QDs; influenza virus A/Yokohama/110/2009 (H3N2) was detected using anti-HA (H3N2) Ab-bioconjugated NPGL and QDs.

2.6. Detection of influenza virus by rapid influenza diagnostic test (RIDT)

To carry out direct and complementary comparison of the detection ability with commercially available influenza diagnostic kit, a commercial RIDT (ImunoAce Flu, TAUNS Lab. Inc., Numazu, Shizuoka, Japan), was purchased to detect Influenza virus A/Yokohama/110/2009 (H3N2) according to manufacturer's protocol. Different virus titers were prepared and then, three drops of virus solution were put on the sample port of the testing kit. Positive and negative influenza diagnostic results were obtained from different significant bands that appeared on the strip paper after 10 min of incubation at room temperature.

3. Results and discussion

3.1. Topographic observation of NPGL films

SEM and AFM images showed that the pore sizes of the substrates varied depending on the dealloying times (Fig. 2a–d). The size of the pores and ligaments increased with longer dealloying times due to increased removal of the less-noble constituent (silver) of the alloy. AFM was used to evaluate the root mean
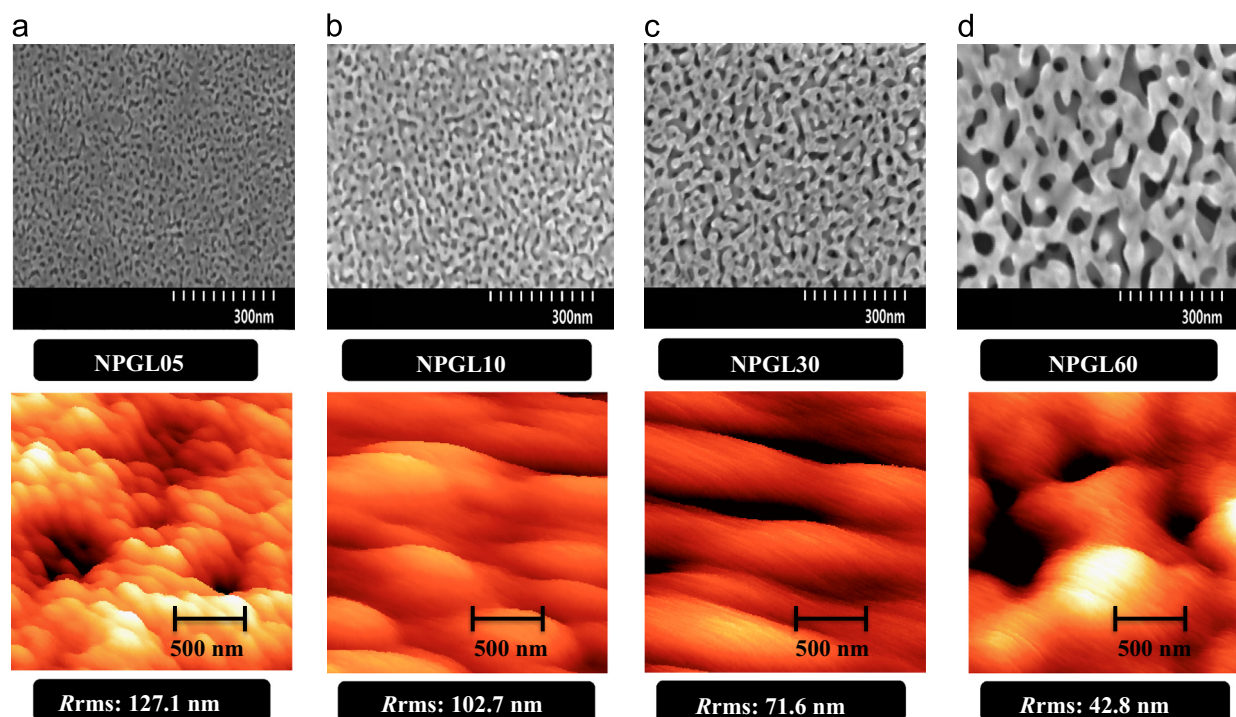
Fig. 2. SEM and AFM images and the measured R_{rms} of each NPGL sample with various dealloying times (5–60 min), where e.g., NPGL05 depicts 5 min of dealloying time. Dealloyed times are 5 min (a), 10 min (b), 30 min (c) and 60 min (d). Bars in upper and lower panels denote 300 and 500 nm respectively.

square roughness (R_{rms}) of the surface of each substrate with different dealloying times. The R_{rms} of the substrate was calculated in the scanning area ($3 \times 3 \ \mu m^2$) of the AFM tip. It was found that the shorter is dealloying times the smaller is pore sizes, resulting in increasing surface irregularities and the surface roughness. Four selected NPGL samples of variant surface roughness (R_{rms} in lower panel of Fig. 2) were used for further optical evaluation.

3.2. Spectroscopic and microscopic studies of the NPGL films

The PL band of the synthesized QD solution was observed at 526 nm with a relative quantum yield of > 20% that was determined from the relative ratio versus rhodamine B dispersed in ethylene glycol, where the quantum yield of rhodamine B was 0.95 (Fig. S1A). Given that the surface roughness of each produced NPGL films differed, special care was taken in the QD immobilizing process to ensure that the equivalent amount of QDs was deposited on each substrate. Consequently, it is important to produce a monolayer of QDs on the surface of a metallic substrate. We monitored the absorbance of the QDs on the respective substrates to maintain similar intensities by adjusting the deposition time during the LbL process. Then, the PL intensity of the QD solution at the same absorption of the LbL film was measured. It was observed that the difference in the PL intensity of the various samples was less than 10%, indicating that fairly identical amount of QDs were deposited on the samples (Fig. S1B).

Indeed, PL enhancement of QDs on metal surfaces was observed. Fig. 3a shows that higher the roughness higher is the PL enhancement; e.g., the emission intensity of QDs on NPGL05 ($R_{rms}=127.1$ nm) and NPGL60 ($R_{rms}=42.8$ nm) was 9- and 2-fold higher than that on a glass substrate, respectively (Fig. 3a). When QDs were deposited on the metal surface without a spacer layer, no PL intensity was observed, rather quenching dominated. This remarkable PL enhancement may be attributed to a strong interaction with surface plasmon of metallic substrate. It has previously been reported that the excitons generated in the QDs can resonate with electron vibrations at the metal surface collectively to induce luminescence enhancement (Lee et al., 2004; Okamoto et al., 2006). Furthermore, the roughness effect on PL enhancement may be related to the multiple scattering phenomena of the SPP mode in combination with rough surfaces. Such roughness and imperfections in nanostructured random media allow SPP of high momentum to scatter and lose momentum and then couple to radioactive light (Okamoto et al., 2006). The fluorescence lifetimes (τ) of the respective samples were measured at an excitation wavelength of 380 nm using a light-emitting diode spectrophotometer (PTI Inc., USA). The spectra in Fig. 3b presents that the rougher the substrate is the shorter is the lifetime, i.e., the PL lifetime varied from 3.17 ns to 1.2 ns while the R_{rms} values varied from 42.8 to 127.1 nm (Fig. 3c). In contrast, the lifetime of CdTe QDs on glass slides was 7.42 ± 0.37 ns. In particular, the short dealloying time generated ultrafine structures that are characterized as small pores and pimples (< 10 nm) that play a major role in plasmonic scattering with consequent PL enhancement. Fig. 3d demonstrates a fluorescence microscopic image of the
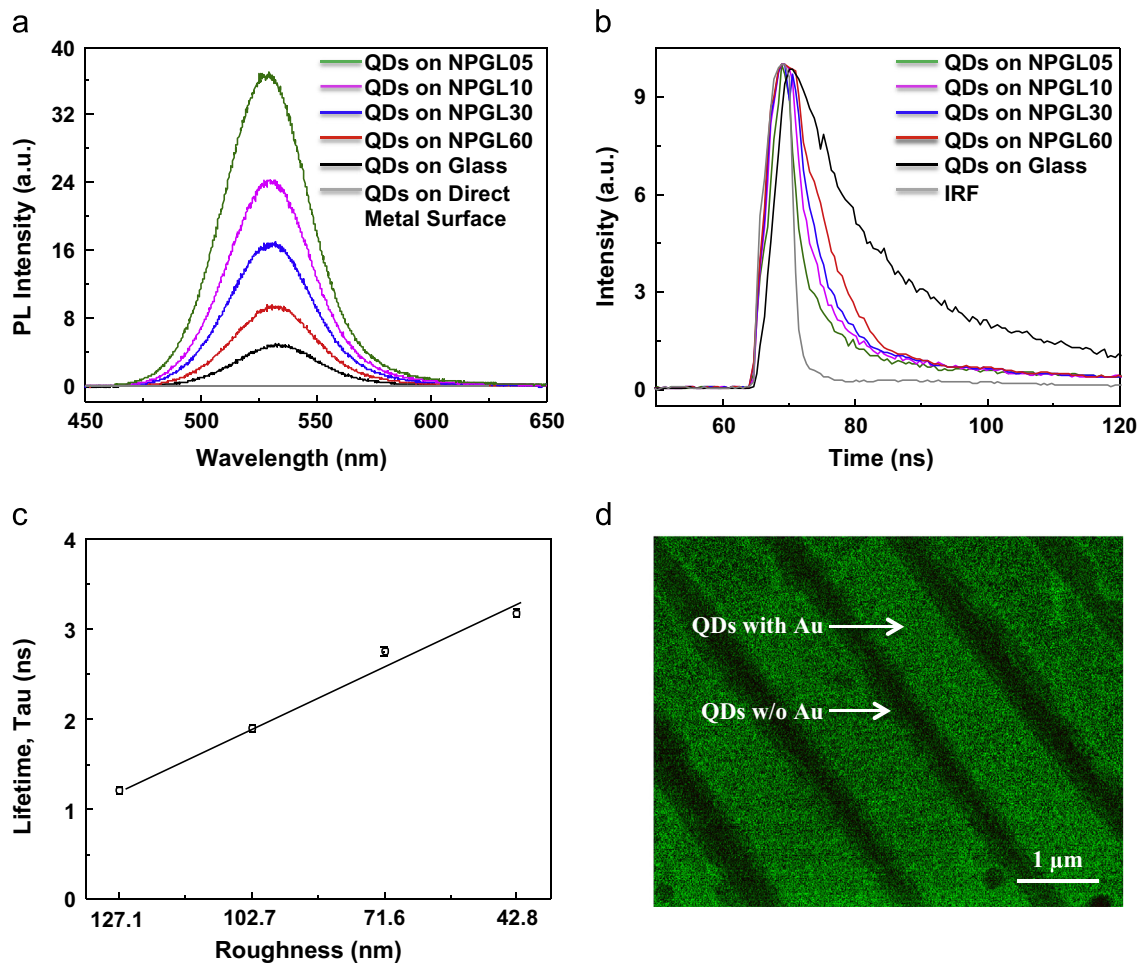
Fig. 3. (a) Photoluminescence (PL) spectra of QDs on different roughnesses of NPGL and glass substrate (for QD only); (b) time-based fluorescence kinetics profile of PL signal for QDs on different surfaces; (c) lifetimes (τ) variance depending on surface roughness; (d) fluorescence microscopic image of QDs on metallic nanostripe patterns. IRF in (b) stands for instrumental response function. The error bars in (c) indicate standard deviation (SD) in each measurement and the scale bar in (d) denotes 1 μm.

QD/polymer-deposited films on metallic nanostripe pattern to demonstrate strong PL enhancement induced by metal enhanced fluorescence. With increasing surface roughness, multiple scattering of lights occurs in nanostructured random media. The high enhancement effect observed in close proximity of metallic nanopatterns is primarily due to the absorption and/or emission bands of the QDs overlap with the scattering wavelength of the rough metallic surface. From these fundamental physical experiments NPGR05 substrate was chosen for further sensing experiments of virus detection.

3.3. Immunoassay of HA on NPGL05 and QDs

It is known that HA, a surface glycoprotein on the surface of viruses has unique immune-specificity in the initial stage of infection mechanism (Wiley and Skehel, 1987). The detailed optical observation at every respective step of bioconjugation with nanomaterials and antibodies was carefully monitored by using ELISA and FTIR spectrophotometry. Immuno-specificity of the anti-HA Ab (ab66189) for influenza virus A/Beijing/262/95 (H1N1) was investigated (Supporting information S1 and S2). A different type of Ab (ab91530) and BSA was used for comparison. A higher absorbance was observed with anti-HA Ab (ab66189) compared to the anti-HA Ab (ab91530) or BSA (Fig. S2A). From these experimental results, anti-HA Ab (ab66189) has a strong immune-specificity for influenza virus A/Beijing/262/95 (H1N1) whereas other antibody and BSA show no binding affinity with influenza A virus. The ELISA test indicated that the antibodies are successfully conjugated on the NPGLs without losing its binding affinity (Fig. S2B and C). Furthermore, FTIR bands found at 3700–3500 cm^{-1} for amide N–H stretching and 1690–1630 cm^{-1} for amide C=O stretching corresponds the chemical binding between NPGL and anti-HA Ab (ab66189) (Fig. S2D).

Then the same experiments were carried out to scrutinize any influence of binding affinity when cysteamine capped QDs were conjugated with anti-HA Ab (ab66189) using recombinant influenza H1N1 HA (New Caledonia/20/1999) (Fig. S3A), resulting that cysteamine capped QDs were successfully conjugated with the antibody (Fig. S3B and C). In fluorescence microscopic image, the aggregated and brighter spot might be virus deposited part on the film (Fig. S3D). The detection procedure consisted of three steps – (i) binding of antibody on NPGL, (ii) binding of antibody on QDs and (iii) immune-reaction between the antibody and antigen.

After confirming the binding affinity of antibody on the surface of NPGL film, the recombinant HA (H1N1) was monitored. Both NPGL film and QDs were bound with anti-HA (H1N1) Ab (ab66189). With HA, these bioconjugated components form a complex, consequently producing high PL intensity from QDs via surface plasmon resonance with the NPGL substrate. In our experiment, 3 times higher PL intensity were monitored in the nanostructure of the antibody-functionalized NPGL than that without the NPGL, where 10 μg/mL of HA was added in each experiment (Fig. 4A). In the quantitative analysis using different concentrations of HA, PL intensities were logarithmically correspondent on HA concentration in the range of 1 ng/ml–10 μg/mL (Fig. 4B and the inset). However, there was no significant PL change without any addition of HA or in the addition of BSA.

3.4. Immunoassay for virus detection

After confirmation of HA monitoring using this novel sensing system with NPGL and QDs, different concentrations of influenza virus A/Beijing/262/95 (H1N1) where the surface of this virus also has specific binding sites of anti-HA (H1N1) Ab were monitored. Similar results were observed as the previous experiment of HA only as shown in Fig. 4b. A significant PL enhancement was observed in the presence of viruses and NPGL (Fig. 5a). Furthermore, a logarithmical relationship existed between PL intensities and the virus concentration in the range of 1 ng/ml–10 μg/mL (Fig. 5b).

Using this developed monitoring system, an influenza virus A/Yokohama/110/2009 (H3N2) was monitored. The specificity of HA (H3N2) Ab 82454 for influenza virus A/Yokohama/110/2009 was confirmed (Fig. 5c), and binding of HA (H3N2) Ab 82454 with NPGL05 and QDs was also confirmed using ELISA (Fig. S4). Then, the sensitivity of influenza virus A/Yokohama/110/2009 (H3N2) detection was observed in the range of 50–10,000 plaque forming units (PFU)/mL (Fig. 5d). The detection limit was shown at ca. 50 PFU/mL.

3.5. Detection of influenza virus using rapid influenza diagnostic test (RIDT)

A commercially available RIDT kit (ImunoAce Flu, TAUNS Lab. Inc., Numazu, Shizuoka, Japan) was used for comparison with our sensing system to diagnose influenza virus infection using the influenza virus A/Yokohama/110/2009 (H3N2). Table 1 shows the results of the RIDT depending on the concentration of virus. In the case of the commercial RIDT, at least 5000 PFU/mL of virus was required for detection, which means the limit of detection (LOD) of the influenza virus detection using our sensing system of NPGL-QDs was 100 times more sensitive than that of the commercial RIDT (Fig. S5).

In this study, a new detection method on metallic surface based on exciton–plasmon interaction was presented. In particular, the
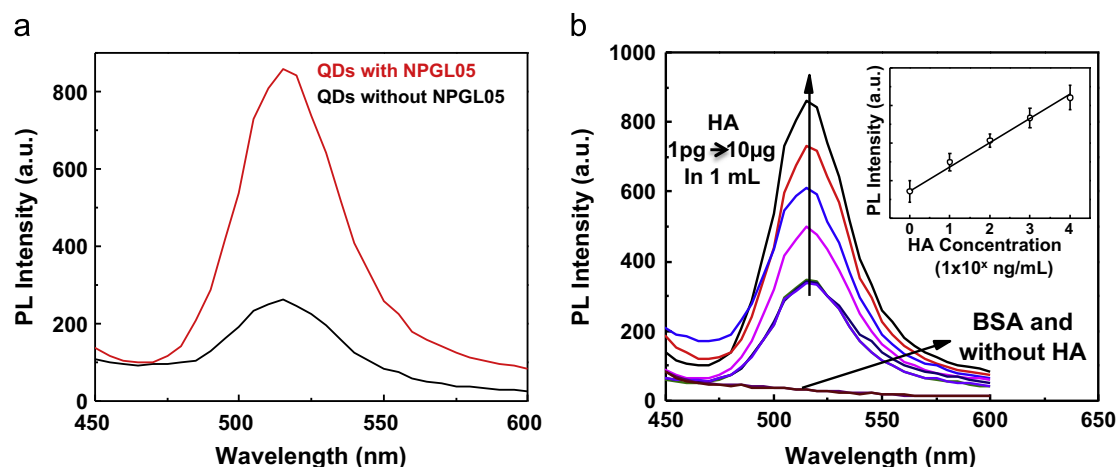
Fig. 4. (a) PL enhancement of QDs with and without the nanostructure; (b) PL enhancement corresponding on different quantities of recombinant influenza HA (H1N1) on anti-HA Ab-conjugated NPGL05. (Inset) The calibration curve of PL intensity versus HA concentration. The error bars indicate SD in each measurement.
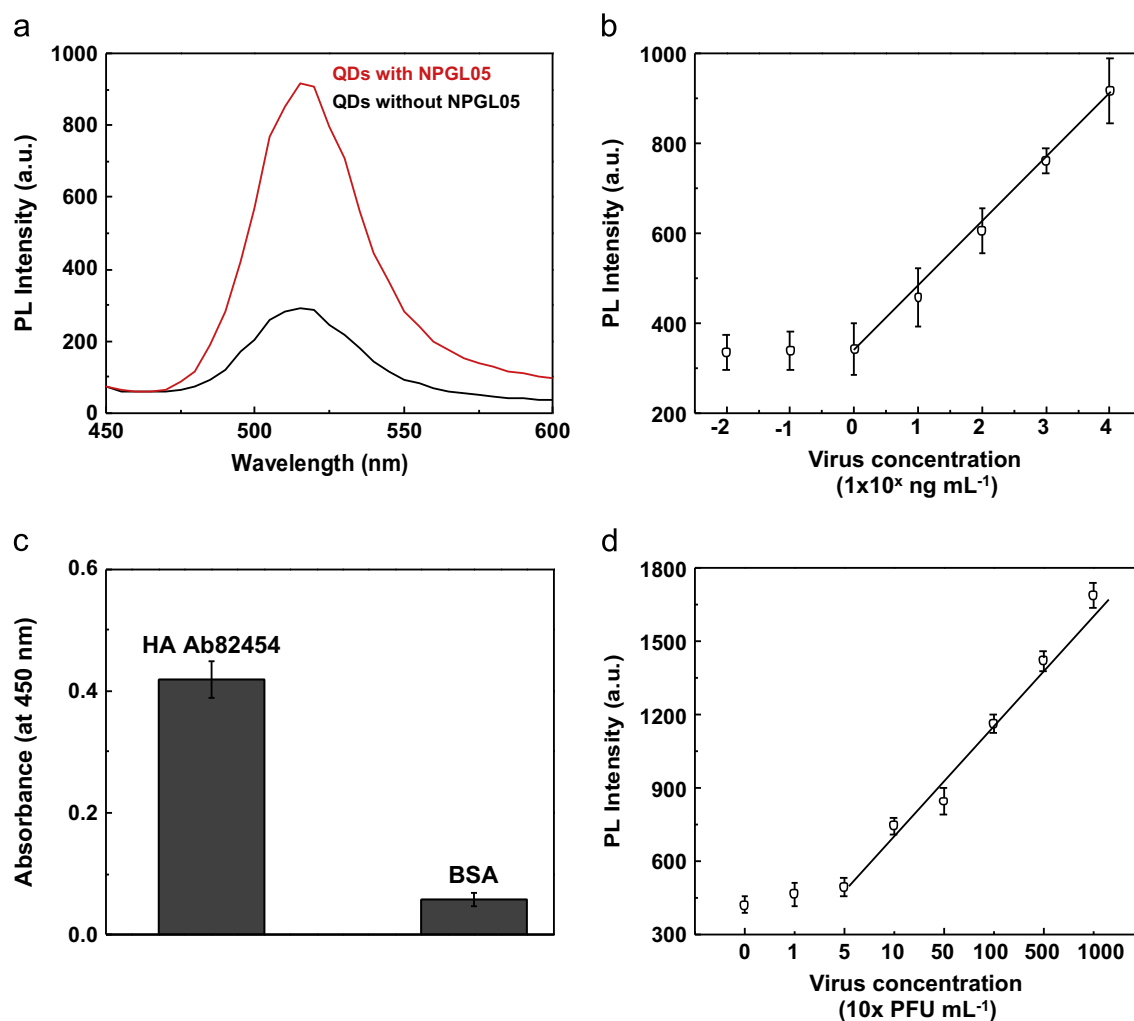
Fig. 5. (a) PL spectroscopic detection of influenza virus A/Beijing/262/95 (H1N1) using anti-HA (H1N1) Ab (ab66189)-bioconjugated QDs depending on the existence of anti-HA (H1N1) Ab (ab66189)-bioconjugated NPGL05 film; (b) PL intensity versus influenza virus A/Beijing/262/95 (H1N1) concentration; (c) ELISA results for anti-HA (H3N2) Ab 82454 binding with influenza virus A/Yokohama/110/2009 (H3N2); (d) the calibration curve of PL intensity corresponding on the concentration of the influenza virus A/Yokohama/110/2009 (H3N2). The error bars in (B–D) indicate SD ($n=3$).

Table 1
Comparison of influenza virus A/Yokohama/110/2009 (H3N2) detection using RIDT.

Detection method	Virus concentration (PFU/mL)								
	10,000	5000	1000	500	100	50	10	1	0
This study	+	+	+	+	+	+	–	–	–
Commercial RIDT	+	+	–	–	–	–	–	–	–

Note: + and – denote the positive and negative diagnoses, respectively.

research centered on the development of robust rough metallic surfaces that would be used for the generation of high efficient optical device for biosensor applications. Many implications for medical take care require a low detection system. An important goal here was to improve detection limit with high sensitivity. As we can see, our proposed detection method showed at least 100 times higher sensitivity than a representative commercial test kit. It might result from the presence of plasmonic rough metallic surface and adjacent control of distance between QDs to induce PL enhancement. In addition, the assay is performed with fewer amounts of reagents and easier to wash out unbound reagents. However, because of the lack of many medical samples, the huge analysis is not attainable using our technique up to now, which will be included in future work.

4. Conclusion

This paper reports a near-field optical evaluation of QDs and plasmonic surface composites with varying roughness. A dramatic enhancement of PL intensity and decay rate of the QDs was achieved on rougher metallic surfaces. The observation of these PL enhancements from nanocomposites was further applied for the development of sensitive influenza virus A (H1N1) detection (up to 1 ng/mL) and influenza A (H3N2) virus isolated from a clinical sample (up to 50 PFU/mL). The proposed method represented an alternative traditional method by requiring a higher sensitivity, much smaller sample volume, less amount reagents. Further research will be focused on the development of rough plasmonic metallic surface using self-assembly techniques as well as clinical evaluation.

Appendix. Supporting information

Supplementary data associated with this article can be found in the online version at http://dx.doi.org/10.1016/j.bios.2014.02.039.

References

Achermann, M., 2010. J. Phys. Chem. Lett. 1, 2837–2843.
Ahmed, S.R., Cha, H.R., Park, J.Y., Park, E.Y., Lee, D., Lee, J., 2012. Nanoscale Res. Lett. 7, 438.
Biener, J., Nyce, G.W., Hodge, A.M., Biener, M.M., Hamza, A.V., Maier, S.A., 2008. Adv. Mater. 20, 1211–1217.
Bonanni, A., Pividori, M.I., del Valle, M., 2010. Analyst 135, 1765–1772.
Choi, Y.J., Kim, H.J., Park, J.S., Oh, M.H., Nam, H.S., Kim, Y.B., Cho, B.K., Ji, M.J., Oh, J.S., 2010. J. Clin. Microbiol. 48, 2260–2262.
Ciesielski, P.N., Scott, A.M., Faulkner, C.J., Berron, B.J., Cliffel, D.E., Jennings, G.K., 2008. ACS Nano 2, 2465–2472.
Deng, Y.M., Caldwell, N., Barr, I.G., 2011. PLoS One 6, e23400.
Detsi, E., Schootbrugge, M., Punzhin, S., Onck, P.R., Hosson, J.T.M.D., 2011. Scr. Mater. 64, 319–322.
Drexler, J.F., Helmer, A., Kirberg, H., Reber, U., Panning, M., Müller, M., Höfling, K., Matz, B., Drosten, C., Eis-Hübinger, A.M., 2009. Emerg. Infect. Dis. 15, 1662–1664.
Driskell, J.D., Jones, C.A., Tompkins, S.M., Tripp, R.A., 2011. Analyst 136, 3083–3090.
Druce, J., Tran, T., Kelly, H., Kaye, M., Chibo, D., Kostecki, R., Amiri, A., Catton, M., Birch, C., 2005. J. Med. Virol. 75, 122–129.
Egashira, N., Morita, S., Hifumi, E., Mitoma, Y., Uda, T., 2008. Anal. Chem. 80, 4020–4025.
Gaponik, N., Talapin, D.V., Rogach, A.L., Hoppe, K., Shevchenko, E.V., Kornowski, A., Eychmüller, A., Weller, H., 2002. J. Phys. Chem. B 106, 7177–7185.
Gramotnev, D.K., Bozhevolnyi, S.I., 2010. Nat. Photonics 4, 83–91.
Huang, J.F., Sun, I.W., 2005. Adv. Funct. Mater. 15, 989–994.
Kawai, Y., Kimura, Y., Lezhava, A., Kanamori, H., Usui, K., Hanami, T., Soma, T., Morlighem, J.E., Saga, S., Ishizu, Y., Aoki, S., Endo, R., Oguchi-Katayama, A., Kogo, Y., Mitani, Y., Ishidao, T., Kawakami, C., Kurata, H., Furuya, Y., Satito, Y., Okazaki, N., Chikahira, M., Hayashi, E., Tsuruoka, S., Toguchi, T., Saito, Y., Ban, T., Izumi, S., Uryu, H., Kudo, K., Sakai-Tagawa, Y., Kawaoka, Y., Hirai, A., Hayashizaki, Y., Ishikawa, T., 2012. PLoS One 7, e30236.
Kok, J., Blyth, C.C., Foo, H., Patterson, J., Taylor, J., McPhie, K., Ratnamohan, V.M., Iredell, J.R., Dwyer, D.E., 2010. J. Clin. Microbiol. 48, 290–291.
Kukol, A., Li, P., Estrela, P., Ko-Ferrigno, P., Migliorato, P., 2008. Anal. Biochem. 374, 143–153.
Lee, J., Govorov, A.X., Dulka, J., Kotov, N.A., 2004. Nano Lett. 4, 2323–2330.
Lee, J., Hernandez, P., Lee, J., Govorov, A.O., Kotov, N.A., 2007. Nat. Mater. 6, 291–295.
Lee, J., Javed, T., Skeini, T., Govorov, A.O., Bryant, G.W., Kotov, N.A., 2006. Angew. Chem. Int. Ed. 45, 4819–4823.
Leong, K., Chen, Y., Masiello, D.J., Zin, M.T., Hnilova, M., Ma, H., Tamerler, C., Sarikaya, M., Ginger, D.S., Jen, A.K.Y., 2010. Adv. Funct. Mater. 20, 2675–2682.
Okamoto, K., Vyawahare, S., Scherer, A., 2006. J. Opt. Soc. Am. B 23, 1674–1678.
Okamoto, K., Niki, I., Shvartser, A., Narukawa, Y., Mukai, T., Scherer, A., 2004. Nat. Mater. 3, 601–605.
Ouyang, J., Chang, M., Zhang, Y., Li, X., 2012. Thin Solid Films 520, 2994–2999.
Owen, T.W., Al-Kaysi, R.O., Bardeen, C.J., Cheng, Q., 2007. Sens. Actuators B – Chem. 126, 691–699.
Panning, M., Eickmann, M., Landt, O., Monazahian, M., Ölschläger, S., Baumgarte, S., Reischl, U., Wenzel, J.J., Niller, H.H., Günther, S., 2009. Eurosurveillance 14, 2003–2008.
Pavlovic, E., Lai, R.Y., Wu, T.T., Ferguson, B.S., Sun, R., Plaxco, K.W., Soh, H.T., 2008. Langmuir 24, 1102–1107.
Perelshtein, I., Applerot, G., Perkas, N., Guibert, G., Mikhailov, S., Gedanken, A., 2008. Nanotechnology 19, 245705–245710.
Rahman, M., Vandermause, M.F., Kieke, B.A., Belongia, E.A., 2008. Diagn. Microbiol. Infect. Dis. 62, 162–166.
Schuller, J.A., Barnard, E.S., Cai, W., Jun, Y.C., White, J.S., Brongersma, M.L., 2010. Nat. Mater. 9, 193–204.
van Elden, L.J., van Essen, G.A., Boucher, C.A., van Loon, A.M., Nijhuis, M., Schipper, P., Verheij, T.J., Hoepelman, I.M., 2001. Br. J. Gen. Pract. 51, 630–634.
Wiley, D.C., Skehel, J.J., 1987. Ann. Rev. Biochem. 56, 365–394.